

Antimicrobial Activity and High Anticorrosion Efficiency of *Carpobrotus acinaciformis* L. Extracts Against C1020 Carbon Steel Corrosion in a Hydrochloric Acid Medium



This work is licensed under a Creative Commons Attribution 4.0 International License

M. Khelifaoui,^{a,b,*} D. Zouied,^{a,b} N. Bouzenad,^{b,c} A. Abdennouri,^{b,c} I. Boussouf,^{a,d} M. Damous,^{b,e} R. N. Boucetta,^{b,f} F. A. Merzeg,^{g,h,i} A. Djermoune,^{g,i} and Y. Belhocine^{b,c}

^aLaboratory LGCES, Faculty of Technology, 20 August 1955 University, El-Hadaeik Road, P.O. Box 26, Skikda 21000, Algeria

^bDepartment of Process Engineering, Faculty of Technology, 20 August 1955 University, P.O. Box 26, Skikda 21000, Algeria

^cLaboratory of Catalysis, Bioprocess and Environment, Department of Process Engineering, Faculty of Technology, University of 20 August 1955, Skikda 21000, Algeria

^dDepartment of Petrochemicals, University of 20 August 1955-Skikda, Skikda, Algeria

^eResearch Unit of Environmental Chemistry and Molecular Structural (CHEMS), University of Constantine 1, Constantine 5000, Algeria

^fLaboratoire de Recherche sur la Physico-Chimie des Surfaces et Interfaces (LRPCSI), University 20 August 1955, Skikda 21000, Algeria

^gScientific and Technical Research Center in Physical and Chemical Analysis (CRAPC), BP 384 Bou-Ismaïl, RP 42004 Tipaza, Algeria

^hResearch Unit in Physico-Chemical Analysis of Fluids and Soils (URAPC-FS), 11 Chemin Doudou Mokhtar, Ben Aknoun, 16028 Alger, Algeria

ⁱTechnical Platform for Physico-chemical Analysis (PTAPC-Bejaia), Targa Ouzemmour, 06000 Bejaia, Algeria

doi: <https://doi.org/10.15255/CABEQ.2024.2397>

Original scientific paper

Received: December 16, 2024

Accepted: March 10, 2025

Corrosion causes significant damage to materials and equipment, prompting the search for effective inhibitors. This study investigates the use of *Carpobrotus acinaciformis* (CA) leaf extracts as alternative corrosion inhibitors for C1020 carbon steel in hydrochloric acid (HCl). Two extraction methods were employed: aqueous (denoted as CAW) and methanolic (denoted as CAM) extracts of *Carpobrotus acinaciformis* leaves. Electrochemical characterization, including polarization curves and electrochemical impedance spectroscopy (EIS), was conducted to evaluate the corrosion inhibition efficiency of the extracts. Additionally, antimicrobial and antifungal activities were assessed against four bacterial strains and one yeast species. Surface and chemical analyses, performed using UV-vis spectroscopy, FTIR, and SEM, demonstrated that the inhibition efficiency (IE) increased with higher inhibitor concentrations. The CAM extract exhibited an inhibition efficiency (IE) of 96.36 % at 350 ppm, while the CAW extract achieved 94.73 % IE at 450 ppm. FTIR analysis identified key functional groups, such as hydroxyl and carbonyl, while SEM analysis confirmed the reduction in corrosion. These findings suggest that CAM and CAW extracts are effective, eco-friendly corrosion inhibitors and antimicrobial agents for C1020 carbon steel in an acidic environment.

Keywords

antimicrobial activity, carbon steel, *Carpobrotus acinaciformis*, extraction, green inhibitor, surface characterization

Introduction

Carbon steel C1020 is recognized for its remarkable mechanical properties, including exceptional toughness, fatigue resistance, high strength, and excellent corrosion resistance. These qualities make it a preferred material in multistage flash desalination and petrochemical industrial plants com-

pared to other steel grades^{1,2}. However, the internal surface of C1020 carbon steel may become coated with a thick layer of inorganic scales and salts due to exposure to circulating cooling water, potentially compromising the functionality of industrial equipment such as cooling towers and boilers³. To address this issue, an effective descaling technique, commonly used in industrial plants, involves cleaning with hydrochloric or sulfuric acids^{3,4}. However, this process often causes corrosion of the steel

*Corresponding author: Malika Khelifaoui
E-mail: m.khelifaoui@univ-skikda.dz

framework, resulting in significant economic damages⁵.

Corrosion of industrial equipment is a critical issue facing both the industry and society, resulting in significant material and equipment damage. Substantial financial resources are spent annually on the maintenance and repair of facilities affected by corrosion-related failures. Therefore, it is essential to prevent corrosion and mitigate its effects⁶. Overdesign, equipment damage, material degradation, and safety concerns are some of the negative consequences of corrosion. Consequently, to prevent corrosion of metal surfaces, acidic environments are typically treated with inhibitors^{7,8}.

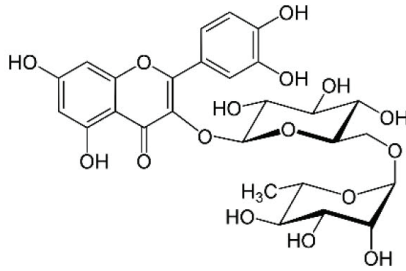
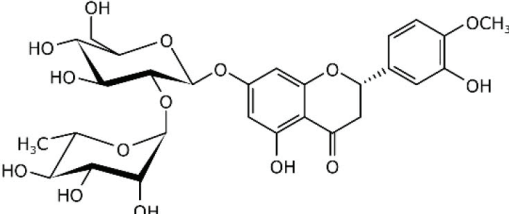
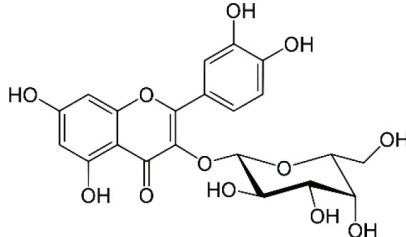
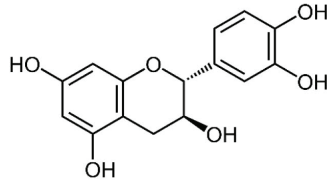
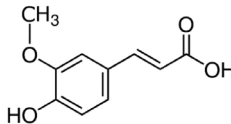
Growing attention is being given to the development of affordable and eco-friendly corrosion inhibitors; as many commonly used industrial inhibitors pose risks to human health and the environment. Most synthetic chemicals are not only costly but also hazardous. As a result, researchers are increasingly focusing on the use of environmentally sustainable corrosion inhibitors^{7,8}. Several studies have shown that plant extracts, containing compounds such as tannins, flavonoids, and alkaloids, are effective in mitigating metal corrosion in acidic environments^{9,10}. These compounds enable plants to inhibit rusting. Due to their diverse range of active properties, plant extracts are used as corrosion inhibitors¹¹. They consist of polar atoms, such as oxygen (O), sulfur (S), phosphorus (P), and nitrogen (N), which are attracted to the metal surface through the adsorption process. These compounds possess lone pairs of electrons, which contribute to the formation of a protective coating on the steel surface¹².

Plant extracts are highly beneficial and play a crucial role in the economy, serving as a source of natural products used to promote human health, particularly over the past decade. They are also employed as antibacterial agents for the treatment of various human diseases¹³. Plant extracts used in traditional medicine contain a wide range of chemicals that can be employed to treat both infectious and chronic diseases¹⁴. *Carpobrotus acinaciformis* L. is a halophyte capable of thriving in highly saline environments. The exceptional ability of halophytes to complete their life cycle in such conditions is attributed to their salt-tolerant or salt-resistant characteristics^{15,16}. *Carpobrotus acinaciformis* L. is a fast-growing, perennial succulent belonging to the Aizoaceae family. It is typically found in Mediterranean climate zones. With its high colonization capacity and ability to thrive in harsh conditions, it is well-adapted to environments characterized by salinity and drought^{16,17}. Species of the *Carpobrotus* genus (CA) are used in various applications, including as preservatives, anti-infective agents, and treatments for conditions such as sinusitis, eczema, and diarrhea. The antioxidant and antibacterial proper-

ties of these species are attributed to flavonoids and phenols, including rutin, neohesperidin, hyperoside, catechin, and ferulic acid,^{18,19} as listed in Table 1. To the best of our knowledge, no scientific studies have specifically addressed the development of anti-corrosion and microbial inhibitors derived from *Carpobrotus acinaciformis* L. extract.

This research aimed to investigate the potential use of *Carpobrotus acinaciformis* leaves, which grow abundantly near Skikda Beach in northern Algeria, as an eco-friendly corrosion inhibitor for C1020 carbon steel in the cooling towers of a petrochemical industrial plant exposed to a hydrochloric acid medium. Two extraction methods were employed: one involving maceration in water at 65 °C, and the other utilizing methanol extraction. Additionally, this study evaluates the potential antimi-

Table 1 – Major chemical structures of CA components^{18,19}

Compound	Structure
Rutin	
Neohesperidin	
Hyperoside	
Catechin	
Ferulic acid	

crobal activities of the plant against Gram-positive (*Bacillus cereus*) and Gram-negative (*Escherichia coli* and *Pseudomonas aeruginosa*) bacteria, as well as the pathogenic fungus *Candida albicans*.

Materials and methods

Specimen and test solution

The carbon steel (C1020) employed to prepare the working electrodes had the following chemical composition (wt%): 98.27 % Fe, 0.36 % Mn, 0.20 % C, 0.02 % Cr, 0.03 % Cu, 0.03 % V, and 0.01 % Mo. A sheet of C1020 carbon steel was cut into pieces measuring 10 mm × 10 mm × 6 mm. To ensure that only one side of each sample was exposed to the electrolyte, the samples were coated with epoxy resin and mounted on copper wires²⁰. The exposed faces of the electrodes were then abraded using abrasive materials of varying grades before each measurement. The electrodes were then carefully dried, washed with distilled water, and degreased with acetone to remove any contaminants²¹. Analytical grade HCl was diluted to prepare corrosive solutions with a concentration of 1 M.

Inhibitor extraction and materials

The preparation of *Carpobrotus acinaciformis* leaf extracts, CAM and CAW, is illustrated in Fig. 1. Leaves of *Carpobrotus acinaciformis* were collected from Skikda Beach, Algeria, dried in the dark for 20 days before being pulverized. To prepare the CAW extract, 30 g of the powdered leaves were mixed with 1 liter of deionized water, heated at 65 °C for 2 hours, and then filtered. The resulting solu-

tion was centrifuged for 10 minutes, followed by further heating at 65 °C for 24 hours to evaporate the water, leaving behind a leaf extract powder. For the CAM extract, 30 g of powdered leaves were mixed with methanol and left to macerate for 24 hours at room temperature. The mixture was then filtered, and the methanol was evaporated using a rotary evaporator.

Characterization of *Carpobrotus acinaciformis* inhibitors

The organic compounds present in *Carpobrotus acinaciformis* leaf extracts, CAM and CAW, were analyzed using Fourier transform infrared (FT-IR) spectroscopy (Perkin Elmer detector), with measurements taken over a wavenumber range of 400 to 4000 cm⁻¹. Additionally, ultraviolet spectrophotometric analysis was performed using a Shimadzu UV-1800 spectrophotometer, with the wavelength range set at 200 to 800 nm.

Electrochemical study

Tafel curves and impedance diagrams were obtained using the “Voltmaster 4” software, which controlled the Voltalab PGZ 301 potentiostat/galvanostat employed in the electrochemical tests. The tests were conducted in double-walled thermostatic corrosion cells²². The CAM and CAW extracts were tested at four different concentrations of inhibitors: 150 ppm, 250 ppm, 300 ppm, and 350 ppm for CAM, and 150 ppm, 250 ppm, 350 ppm, and 450 ppm for CAW. The PGZ 301 system included a metal working electrode (1 cm²), a platinum counter electrode, and a saturated calomel electrode (SCE) as the reference electrode.

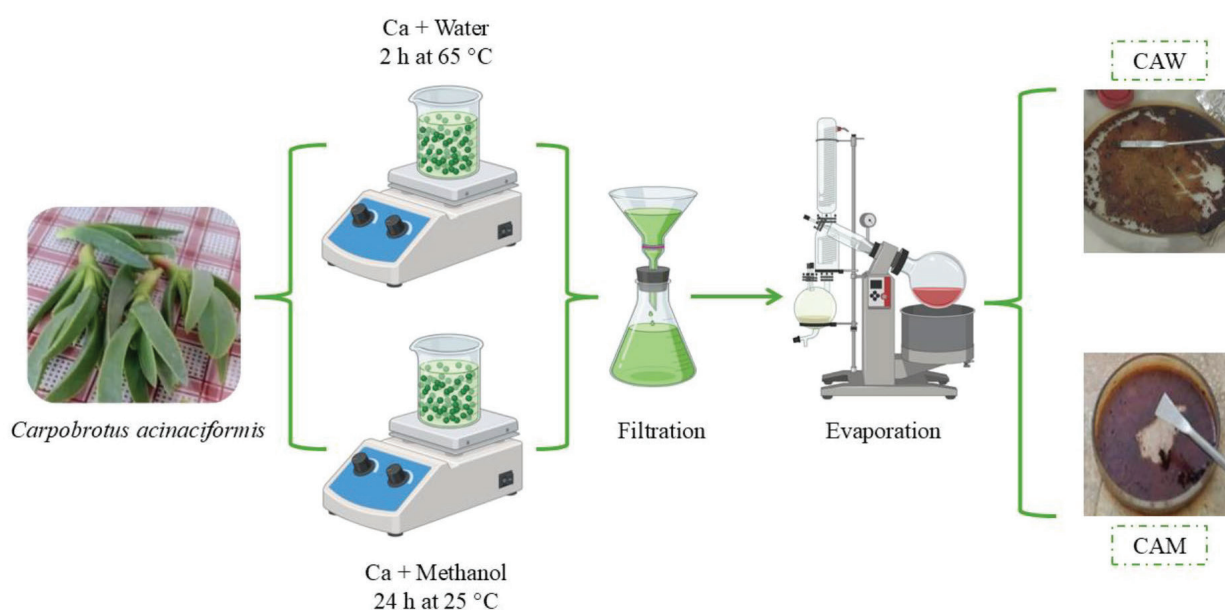


Fig. 1 – Extraction of inhibitors from *Carpobrotus acinaciformis* leaves

An aggressive solution of 1 M HCl was applied to the working electrode for 30 minutes to allow the system to reach a steady-state open circuit potential (OCP). Tafel polarization plots were obtained by sweeping at a rate of 1 mV s^{-1} , within a voltage range from -200 mV to -700 mV , using a 10 mV peak-to-peak wave voltage. Nyquist curves were recorded at OCP, with frequencies ranging from 100 kHz to 10 mHz . After 30 minutes, all assessments were regulated by computer software at the resting potential, with potential values recorded relative to the saturated calomel electrode (SCE). Electrochemical impedance spectroscopy data were analyzed using EC-Lab software^{22,23}.

Surface morphology study

The $1 \text{ cm} \times 1 \text{ cm}$ polished mild steel samples were highly reflective, resembling a mirror finish. These samples were immersed in 350 ppm of CAM, 450 ppm of CAW inhibitor, and a blank solution for a duration of 24 hours. After the experiment, a scanning electron microscope (SEM) was used to assess the surface characteristics and elemental composition of the specimens²⁴.

Antimicrobial and antifungal activities assay

The antimicrobial and antifungal effects of *Carpobrotus acinaciformis* L. extracts, prepared using water (CAW) and methanol (CAM), were evaluated against four bacterial strains and one yeast, *Candida albicans* ATCC®10231, obtained from the American Type Culture Collection (ATCC). The strains included one Gram-positive bacterium (*Bacillus cereus* ATCC®10876), and three Gram-negative bacteria (*Pseudomonas aeruginosa* ATCC®27853, *Klebsiella pneumoniae* ATCC®700603, and *Escherichia coli* ATCC®25922). An agar diffusion meth-

od was used to assess the inhibitory activity of the *Carpobrotus acinaciformis* L. extracts. Each bacterial strain was cultured in a nutrient broth for 18 hours at $37 \text{ }^\circ\text{C}$. After incubation, the bacterial cultures were transferred to a 0.9% NaCl solution and adjusted to an optical density (OD) of $0.08\text{--}0.10$ at 600 nm . Muller-Hinton agar plates were then uniformly re-inoculated using a sterile swab. Plant extract solutions were prepared using 99.9% pure dimethyl sulfoxide (DMSO), and subsequently diluted in a 2.048 fold series, ranging from the initial concentration to $15 \mu\text{g mL}^{-1}$. Disks impregnated with varying amounts of the extracts were placed onto the agar plates and incubated for 24 hours at $37 \text{ }^\circ\text{C}$. The inhibition zones around the disks were measured to evaluate the antimicrobial activity²⁵.

Results and discussion

FT-IR and UV-Vis analysis

FTIR spectroscopy was employed to identify the functional groups in the CAM and CAW extracts. The FTIR spectra of the CAW and CAM extracts are shown in Fig. 2. The absorption bands at 3329 cm^{-1} for CAM and 3363 cm^{-1} for CAW, corresponding to the OH stretch (phenol), confirm the presence of phenolic compounds in both extracts. A C=C stretch, characteristic of alkenes, was observed at 1522 cm^{-1} , present only in the CAW extract. The carbonyl group (C=O) in the polyphenolic compounds of CAM was found at 1613 cm^{-1} and 1642 cm^{-1} . The aromatic ring was identified at 1430 cm^{-1} in both CAM and CAW. The C–O stretch for the carbonyl group appeared at 1070 cm^{-1} for CAM, and 1053 cm^{-1} for CAW. Additionally, a peak at 2322 cm^{-1} , linked to the presence of carboxylic acid groups (–COOH), was observed in both extracts.

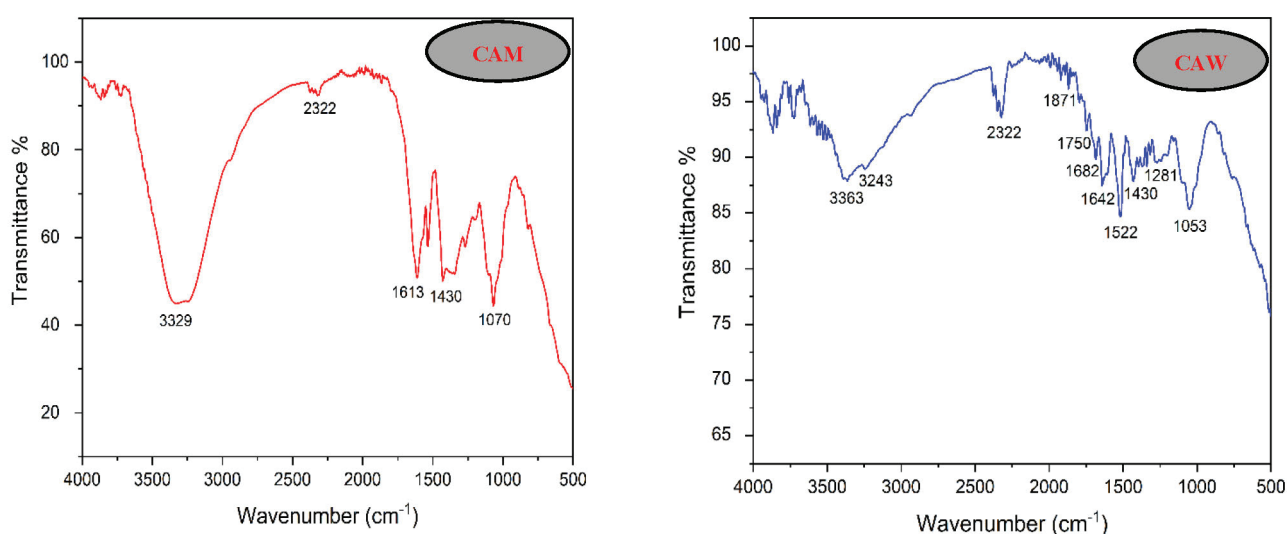


Fig. 2 – FT-IR spectrum of (CAM) and (CAW) extracts

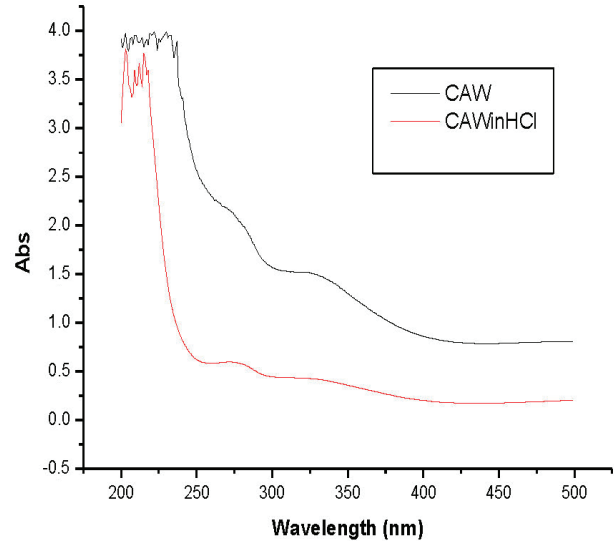
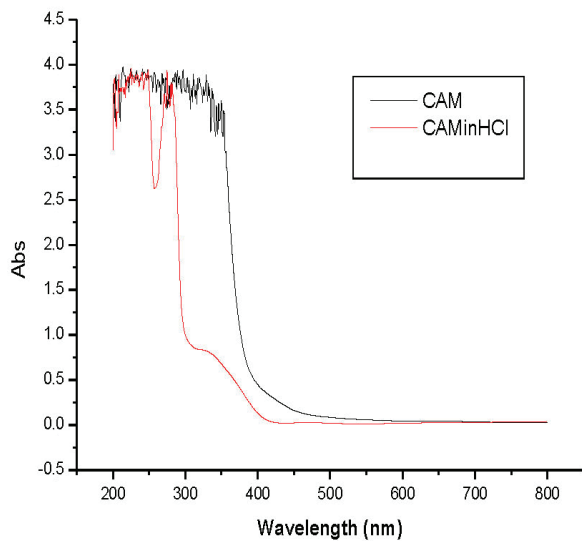


Fig. 3 – UV-Vis spectrum of (CAM) and (CAW) extracts

For further analysis, the structures of the CAM and CAW leaf extracts were examined using UV-Vis spectroscopy.

Fig. 3 displays the UV-visible spectra of the CAM and CAW inhibitors before and after 24 of immersion of C1020 carbon steel in solutions containing 340 ppm of CAM and 450 ppm of CAW. In both cases, a noticeable decrease in absorbance intensities was observed. This reduction was attributed to interactions between *Carpobrotus acinaciformis* L. molecules and the C1020 surface, leading to a decrease in adsorption intensity and displacement of adsorption bonds. These results strongly support the formation of a complex between Fe^{2+} ions and the components of CAM and CAW in the 1 M HCl solution, which subsequently adsorbed onto the surface of C1020 carbon steel.

Potentiodynamic polarization curves

Potentiodynamic polarization curves for C1020 carbon steel were measured in a 1 M HCl acidic environment, both with and without different concentrations of CAM and CAW. The measurements were conducted at a temperature of $298 (\pm 1)$ K. Fig. 4 presents the Tafel curves obtained under these conditions, along with key corrosion parameters, including corrosion potential (E_{corr}), corrosion current densities (I_{corr}), corrosion kinetics (β_a and β_c , determined by extrapolating the anodic and cathodic slopes of the Tafel curves). The inhibition efficiency (IE_p %) was calculated using the following equation (1).

$$IE_p (\%) = \frac{I_{\text{corr}}^{\circ} - I_{\text{corr}}}{I_{\text{corr}}^{\circ}} \cdot 100 \quad (1)$$

Where I_{corr}° and I_{corr} represent the corrosion current densities in the absence and presence of the inhibitor, respectively.

Fig. 4 illustrates a significant decrease in current density due to the presence of CAM and CAW inhibitors. The polarization parameters, both with and without the inhibitors, are provided in Table 2. As shown in Fig. 4 and Table 2, CAM and CAW inhibitors effectively slowed the corrosion of steel without altering the overall behavior of the Tafel lines. This effect was attributed to the inhibitors preventing active areas on the steel surface through their electron-rich adsorption centers. The polarization curves indicated that the presence of CAM and CAW altered both the anodic and cathodic Tafel slopes when compared to the inhibitor-free solution. This suggested that CAM and CAW act as mixed-type inhibitors. Additionally, the anodic curves revealed the formation of compounds on the metal surface, which were likely associated to the development of iron(II) complexes on the C1020 steel surface²⁶. Another important aspect was the variation in the corrosion potential (E_{corr}), which provided valuable insights into the inhibitor type. A change in the corrosion potential value exceeding 85 mV is typically interpreted as indicative of an inhibitor exhibiting a specialized inhibitory effect on either the cathodic or anodic reaction^{27,28}.

In the present case, CAM and CAW can be classified as mixed-type inhibitors, as evidenced by a shift in the corrosion potential of less than -85 mV. This suggests that both the cathodic reaction, involving oxygen reduction and hydrogen evolution under acidic conditions, and the primary anodic reaction, which governs the dissolution of steel, were simultaneously inhibited. The observed reduction in corrosion rates was attributed to the adsorption of CAM and CAW molecules at both anodic and cathodic sites²⁹ on the steel surface.

Moreover, the simultaneous alteration of both the anodic and cathodic Tafel curves suggested that

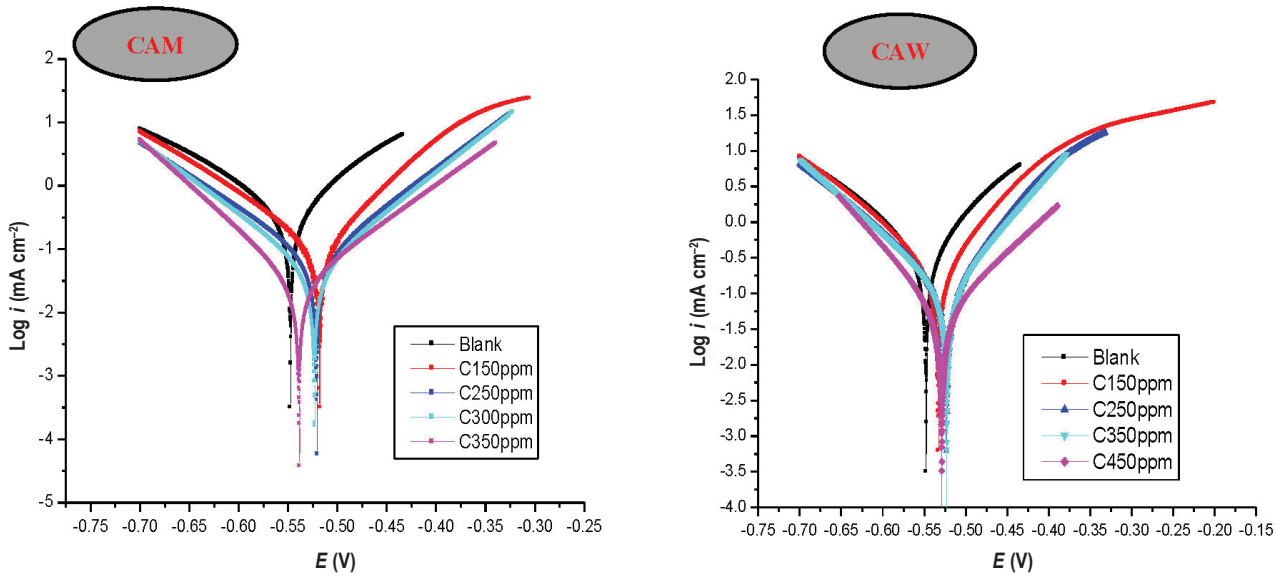
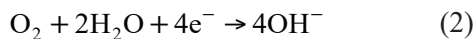


Fig. 4 – Potentiodynamic polarization patterns for C1020 steel with various doses of CAM and CAW in 1 M HCl at 298 K

the presence of the inhibitors did not interfere with the metal dissolution mechanism itself, but rather activated the inhibition process.

In the HCl solution, the reduction of oxygen is the primary cathodic corrosion reaction:



The anodic dissolution reaction of carbon steel:

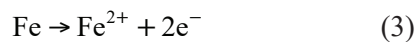


Table 2 illustrates that the corrosion current density decreased in the presence of CAM and CAW inhibitor concentrations, with the maximum reduction observed at 350 ppm for CAM and 450 ppm for CAW. The inhibition efficiency increased with the concentration of CAM and CAW inhibitors, reaching peak values of 94.66 % and 90.61 %, respectively. These results demonstrate that the chemical inhibitors exhibited strong adsorption charac-

teristics, with an increasing number of inhibitor molecules adsorbing onto the iron surface. As the inhibitor concentration increased, more molecules were attracted to the surface, leading to a more effective surface coverage and enhanced corrosion protection³⁰.

Electrochemical impedance spectroscopy (EIS)

Electrochemical impedance measurements provide essential insights into the processes and reaction kinetics at the metal/electrolyte interface. These measurements allow for the identification of relaxation times, with rapid processes occurring at high frequencies and slower steps, such as transport or diffusion, taking place at lower frequencies³¹.

Fig. 5 and Fig. 6 display the impedance data for C1020 steel samples in 1M HCl solutions, both before and after the addition of varying CAM and CAW concentrations. Fig. 5 highlights the Nyquist

Table 2 – Corrosion characteristics and inhibitory efficiency of C1020 steel with various doses of CAM and CAW in 1 M HCl at 298 K

	C (ppm)	E_{corr} (mV)	I_{corr} (mA cm ⁻²)	β_c (V dec ⁻¹)	β_a (V dec ⁻¹)	IE_p (%)
Blank	00	-547.60	0.600	137.2	119.5	/
CAM	150	-518.30	0.105	96.4	72.5	82.50
	250	-521.09	0.059	92.6	82.6	90.16
	300	-522.00	0.048	88.2	81.0	92.00
	350	-536.49	0.032	66.3	92.9	94.66
CAW	150	-532.51	0.155	87.0	69.0	74.11
	250	-522.80	0.140	105.5	82.3	76.65
	350	-552.76	0.108	96.6	75.6	81.87
	450	-528.89	0.056	76.9	94.3	90.61

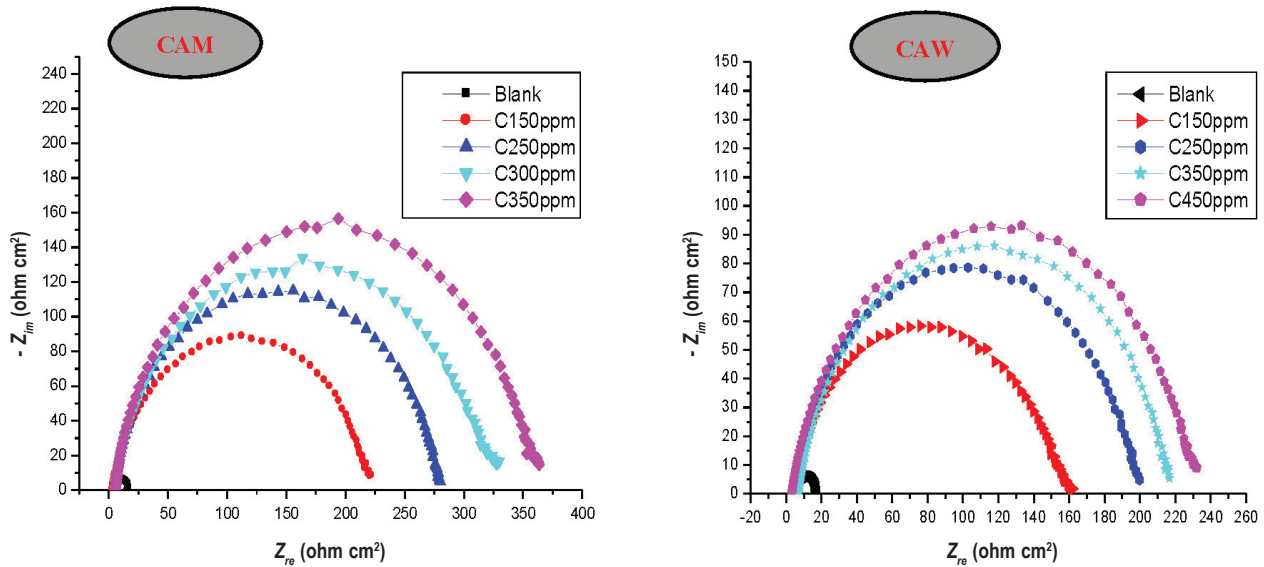


Fig. 5 – Nyquist diagrams of C1020 steel with various concentrations of CAM and CAW in 1 M HCl at 298 K

plots, and Fig. 6 presents the Bode modulus and phase angle for the CAM and CAW inhibitors.

For all tested concentrations of CAM and CAW inhibitors, the Nyquist plots exhibited an identical shape, suggesting that the corrosion mechanism remained unchanged²⁸. A single time constant was observed in the corresponding EIS spectra, indicating that charge transfer was the primary mechanism governing corrosion, both in the presence and absence of varying CA extract doses. The charge transfer mechanism was likely associated with the high frequency capacitive loops. The variation in impedance between lower and higher frequencies can be used to calculate the diameters, which are related to charge transfer resistance (R_{ct})³².

A continuous enlargement of the loops demonstrates an increasing trend in charge transfer resistance with rising CA concentration. Given that the spectra contained only a single time constant, it can be inferred that the active ingredients in the CA extract hindered the corrosion reaction by obstructing the active sites, thus interfering with the charge transfer process. A thorough examination of Fig. 5 reveals that the presence of the CA extract caused an increase in phase angles, indicating capacitive behavior. Nyquist plots were also employed to display damped semicircles. According to Hamed *et al.*³³ and Kherraf *et al.*²⁰ surface roughness, inhibitor adsorption, and surface contaminants all contribute to frequency depression, which is represented as a variation from a perfect circular form. Fig. 7 depicts an R (RQ) equivalent circuit, which is commonly used to represent impedance spectra with a single time constant. The results were analyzed using EC-Lab software, yielding values for solution resistance (R_s), charge transfer resistance (R_{ct}), and constant phase element (CPE_{dl}), which characterizes the dou-

ble-layer capacitance (C_{dl}), as highlighted in Fig. 7, with additional results presented in Table 3. The (CPE_{dl}) includes two additional parameters: the exponent (n) and admittance (Y_0).

The parameter n served as a suitable measure of the surface condition, ranging from 0 to 1. For more homogeneous electrode surfaces, the parameter n approaches 1³². Fig. 7 helps in assessing the precision and accuracy of the fitted results with the proposed electrical circuit. Table 3 lists the parameters extracted from the EIS data, both with and without the CA plant extracts. Inhibition efficiency (E_{EIS}) and double-layer capacitance (C_{dl}) were calculated using Equations (4) and (5).

$$E_{EIS} (\%) = \frac{R_{ct} - R_{ct}^0}{R_{ct}} \cdot 100 \quad (4)$$

$$C_{dl} = Y_0 (2\pi f_{max})^{n-1} \quad (5)$$

In Equation (4), E_{EIS} represents the inhibition efficiency, where R_{ct}^0 and R_{ct} denote the charge transfer resistances without and with the CA extract, respectively. Equation (5) provides the double-layer capacitance C_{dl} , and f_{max} is the frequency at which the imaginary component of the impedance reached its maximum.

As highlighted in Table 3, with the increasing doses of CA extract, both the inhibitory efficiency and the polarization resistance exhibited an increasing trend. Additionally, by evaluating the n parameter using the EIS data, the heterogeneity of the surface could be further investigated, allowing for a better understanding of both the inhibitor adsorption and the metal dissolution processes on the metal surface. Table 3 demonstrates that an increase in the concentration of each inhibitor resulted in a rise in inhibition efficiency. At 350 ppm, CAM showed a

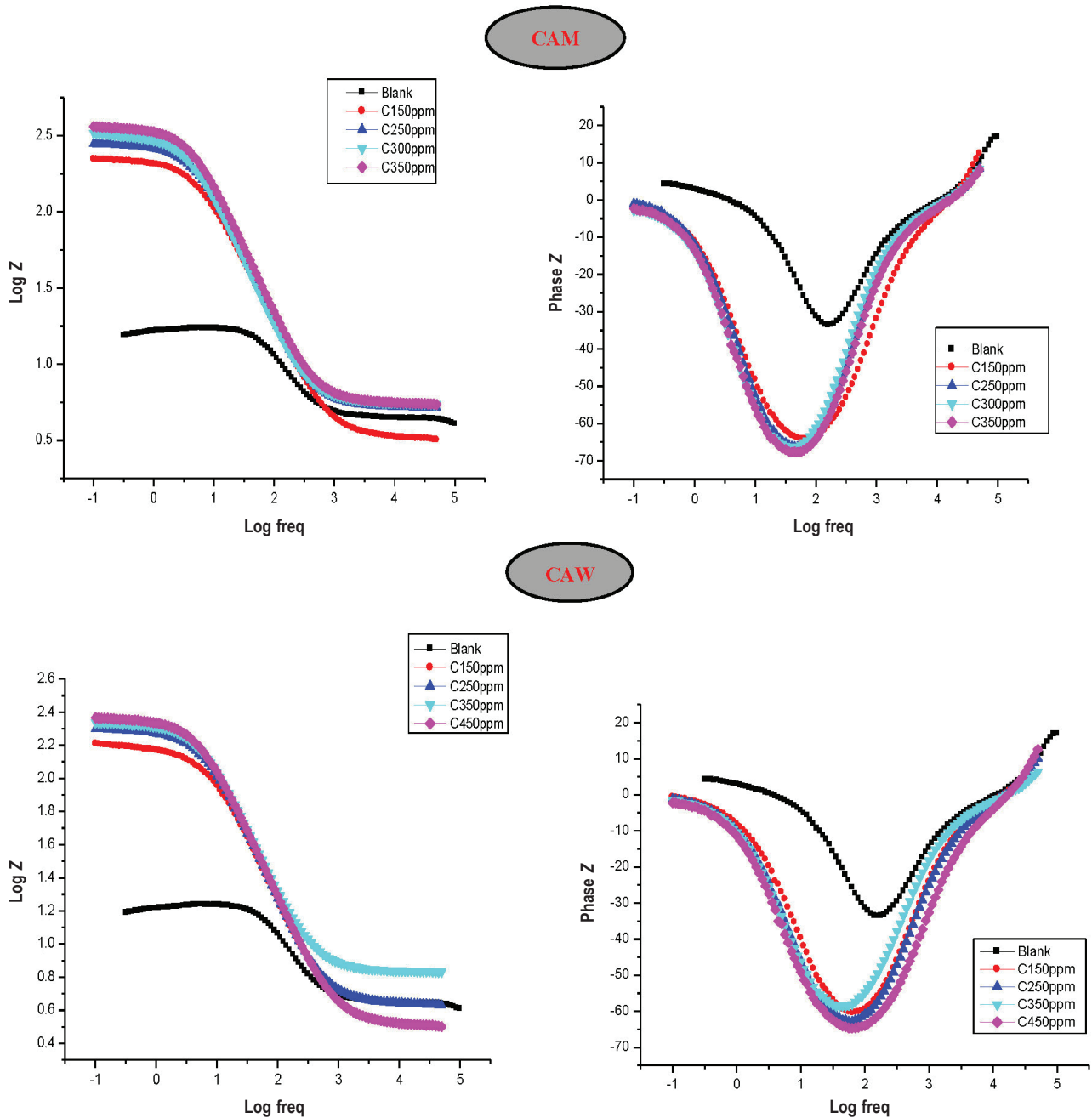


Fig. 6 – Bode modulus and Bode phase angle plots of CAM and CAW inhibitors for carbon steel C1020 in 1 M HCl

maximum inhibitory efficiency of 98.01 %, while the CAW extract exhibited a maximum inhibitory efficiency of 94.05 % at the same concentration. These findings indicate that the CAM inhibitor outperformed the CAW extract in terms of inhibitory efficiency, suggesting that the protective properties of the film layer formed on the surface of C1020 carbon steel had been enhanced with the introduction of CAM and CAW inhibitors in 1 M HCl solutions³⁴. As the amount of CA extract increased, the n value approached 1. This suggests that samples exposed to uninhibited solutions were more susceptible to corrosion, leading to a rougher surface com-

pared to those subjected to inhibited solutions. This effect likely resulted from the uniform corrosion protection provided by the adsorption of CA molecules onto the metal surface.

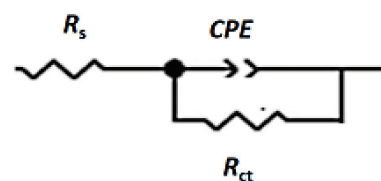


Fig. 7 – Equivalent circuit for impedance data fitting with and without CAM and CAW

Table 3 – Impedance parameters and inhibition efficiency of C1020 steel with various doses of CAM and CAW in 1 M HCl at 298 K

	C (ppm)	R_s (Ω cm ²)	CPE_{dl} (F cm ⁻²)	n	R_{ct} (Ω cm ²)	E_{EIS} (%)
Blank	00	4.429	$0.194 \cdot 10^{-3}$	0.953	12.84	/
	150	3.259	$0.207 \cdot 10^{-3}$	0.866	217.50	94.09
	250	5.241	$0.159 \cdot 10^{-3}$	0.909	271.20	95.26
	300	5.555	$0.170 \cdot 10^{-3}$	0.908	312.30	95.88
	350	5.560	$0.139 \cdot 10^{-3}$	0.908	353.40	96.03
CAM	150	4.317	$0.209 \cdot 10^{-3}$	0.750	148.40	91.61
	250	4.329	$0.198 \cdot 10^{-3}$	0.878	193.30	93.35
	350	6.829	$0.202 \cdot 10^{-3}$	0.867	210.70	93.90
	450	3.240	$0.202 \cdot 10^{-3}$	0.866	228.10	94.37
	CAW					

In general, as the amount of each studied inhibitor increased, the C_{dl} values decreased. This decline in C_{dl} was attributed to the reduction in the local dielectric constant, as the active components of CA replaced water molecules on the sample surface. The addition of the inhibitor enhanced adsorption on the metal surface by forming a protective layer, which can be explained by the adsorption of the leaf components onto the electrode surface³⁵. As a result, there was less electron transfer between the corrosive solution and the metal surface. The formation of these films on the carbon steel surface gradually replaced the water molecules, leading to a reduction in metal dissolution and a shift in C_{dl} values.

Isotherm of adsorption

The adsorption capability at the metal/solution interface is the primary factor determining the effectiveness of a corrosion inhibitor. Inhibitor molecules often replace water molecules adsorbed on a metal surface in a displacement process. Adsorption can be classified as either chemical or physical. Understanding the nature of this adsorption process is crucial, as it provides insights into the inhibitor-metal surface interaction^{31,36}. Many adsorption isotherms were tested to evaluate the adsorption behavior of CAM and CAW on the surface of C1020 steel in a 1 M HCl solution. The Langmuir adsorption isotherm provided the best fit for the various inhibitors under study.

The following Equations (6) and (7)²¹ present the Langmuir isotherm. The standard free energy of adsorption (ΔG_{ads}°) can be obtained using Equation (8)^{37,38}

$$\frac{C_{inh}}{\theta} = \frac{1}{K_{ads}} + C_{inh} \quad (6)$$

$$\theta = \frac{R_{ct(inh)} - R_0}{R_{ct(inh)}} \quad (7)$$

$$\Delta G_{ads}^{\circ} = -RT \ln(1000 K_{ads}) \quad (8)$$

Where, C_{inh} represents the inhibitor concentration, K_{ads} is the adsorption equilibrium constant, θ denotes surface coverage, 1000 refers to the concentration of water molecules expressed in units of g L⁻¹. R is the universal gas constant, and T is the temperature.

Fig. 8 displays the correlation between C_{inh}/θ and C_{inh} at 298 K for CAM and CAW inhibitors.

The relationship between C_{inh}/θ and C_{inh} followed a linear trend, with regression coefficients (R) of 0.999 and 1 for CAM and CAW, respectively. The slope and interception were determined, with the slope being 1.083 for CAM, and 1.045 for CAW. The slope was close to unity for both inhibitors. This slight divergence could be attributed to the binding of the adsorbed species on the metal's outer layer, which may occur through mutual repulsion or attraction³⁹. These findings support the adsorption of the inhibitors on the steel surface, consistent with the Langmuir adsorption isotherm, which assumes no interaction between the adsorbed molecules.

Table 4 presents the calculated free energy of adsorption (ΔG_{ads}), which was -29.09 kJ mol⁻¹ for the CAM inhibitor and -29.45 kJ mol⁻¹ for the CAW inhibitor. The negative values of ΔG_{ads} indicate the spontaneity of the adsorption process and the stability of the adsorbed layer on the metallic surface. These values suggest that the adsorption of the inhibitor compounds onto the carbon steel electrode occurred primarily through physical adsorption. According to previous studies, ΔG_{ads}° values below -40 kJ mol⁻¹ are indicative of chemisorption, while values between -20 and -40 kJ mol⁻¹ suggest

Table 4 – Adsorption free energy values for CAM and CAW inhibitors at 298 K from impedance plots

Inhibitors	ΔG_{ads} (kJ mol ⁻¹)
CAM	-29.09
CAW	-29.45

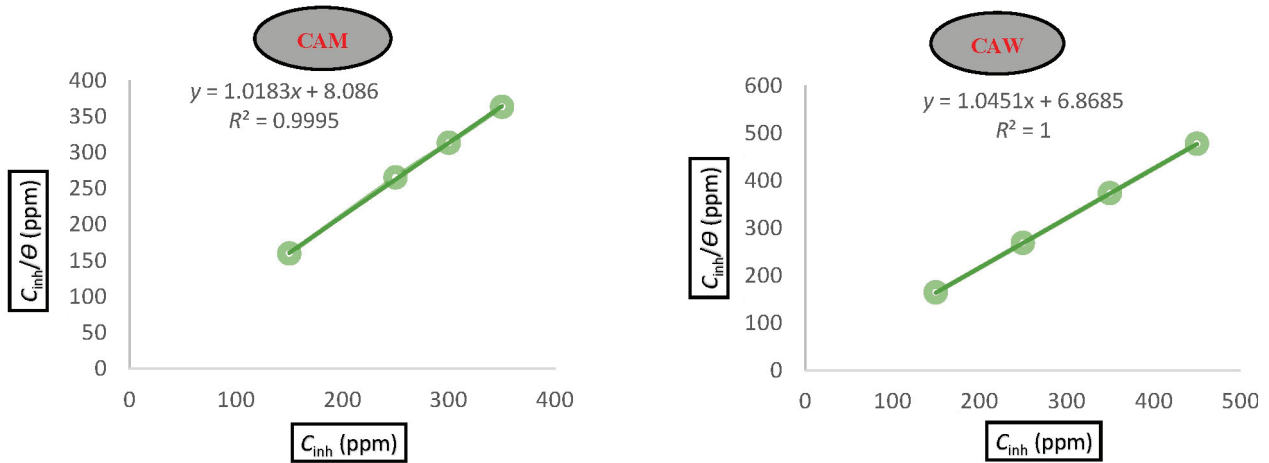


Fig. 8 – Langmuir adsorption isotherms of CAM and CAW on the surface of carbon steel C1020 in 1 M HCl at 298 K

electrostatic interactions or physical adsorption²¹. In this study, the calculated ΔG_{ads} values fell within the range of -20 to -40 kJ mol^{-1} , confirming that both chemical and physical interactions governed the adsorption mechanism for the CAM and CAW inhibitors.

Surface morphology

Surface morphology of metals and alloys has been extensively studied using scanning electron microscopy (SEM)²⁹. After 24 hours of immersion in 1 M HCl, the surface morphology of C1020 steel

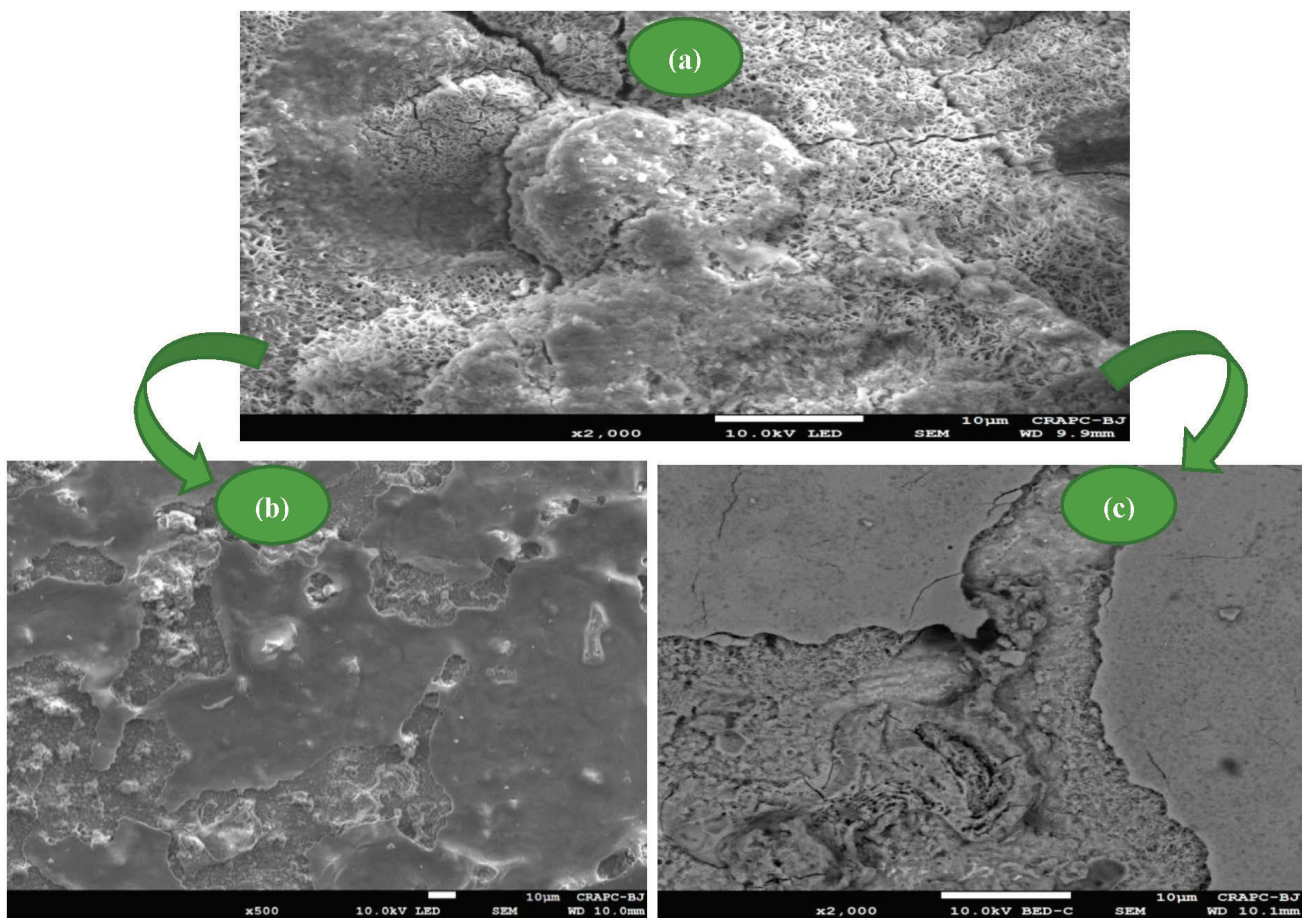


Fig. 9 – SEM graphs of C1020 carbon steel specimen after immersion in HCl (1 M) solution at 25 °C for one day: (a) without inhibitor; (b) 350 ppm of CAM, (c) 450 ppm of CAW

was analyzed with and without the presence of 350 ppm CAM, and 450 ppm CAW inhibitors at room temperature (Fig. 9). The unprotected steel surface (Fig. 9a) exhibited noticeable damage due to corrosion caused by the acidic medium. In contrast, the surfaces treated with CAM and CAW inhibitors (Fig. 9b and 9c) displayed smoother surfaces, indicating the protective effect of the inhibitors. In the absence of inhibitors, the steel surface exhibited generalized corrosion, accompanied by a thick and uneven corrosion product layer. In contrast, when CAM and CAW inhibitors were present, a more localized corrosion pattern was observed, accompa-

nied by the formation of a thin, uniform protective layer on the steel surface. This layer effectively shielded the metal from the HCl solution, reducing permeability and confirming the inhibitors' protective effect, as demonstrated by the electrochemical test results. These findings are consistent with the outcomes of the electrochemical investigations.

Antimicrobial and antifungal effects

The results in Table 5 and Fig. 10 show the inhibition diameters of plant extracts from *Carpobrotus acinaciformis* L., using water (CAW) and methanol (CAM) as solvents, on four bacterial strains

Table 5 – Antibacterial effect of CAW and CAM extracts against different bacterial strains at different concentration

Sample	Bacteria	Inhibition diameter (mm)							
		Concentration							
		2048 $\mu\text{g mL}^{-1}$							
CAW	<i>E. coli</i>	20.66±0.33	18.25±1.09	17.33±0.35	16.00±0.50	15.00±0.35	14.00±0.57	13.25±0.55	11.00±0.33
CAM		20.75±1.11	20.00±1.09	17.75±0.35	16.25±0.66	15.75±0.75	14.75±0.85	13.75±0.35	13.50±0.50
CAW	<i>K. pneumoniae</i>	18.50±1.09	16.25±0.33	15.75±0.75	15.00±0.95	14.50±1.20	14.00±1.09	13.25±0.75	11.25±0.33
CAM		20.00±1.35	18.75±0.95	17.25±1.11	16.00±1.16	14.75±0.85	14.00±0.57	12.25±0.85	12.00±0.35
CAW	<i>B. cereus</i>	16.75±1.35	16.25±1.01	15.75±0.89	15.25±1.09	15.00±1.16	14.75±0.75	14.25±0.33	13.25±0.55
CAM		22.75±1.19	22.00±0.75	16.75±0.75	16.25±0.66	15.50±0.85	13.75±0.57	13.25±0.66	12.00±0.35
CAW	<i>P. aeruginosa</i>	19.75±1.33	17.50±0.89	16.50±0.66	16.00±0.35	14.75±0.95	13.50±0.66	13.00±0.56	11.25±0.33
CAM		24.00±1.09	19.75±0.95	17.25±0.35	15.50±0.95	15.00±0.57	13.50±0.85	13.00±0.35	12.75±0.50
CAW	<i>C. albicans</i>	20.75±1.36	19.25±1.33	17.50±1.16	15.00±0.66	14.25±0.66	12.75±0.71	11.25±0.33	10.50±0.35
CAM		21.33±1.17	20.00±0.89	17.75±0.33	17.00±0.33	16.50±0.33	15.25±0.57	14.00±0.35	13.25±0.33

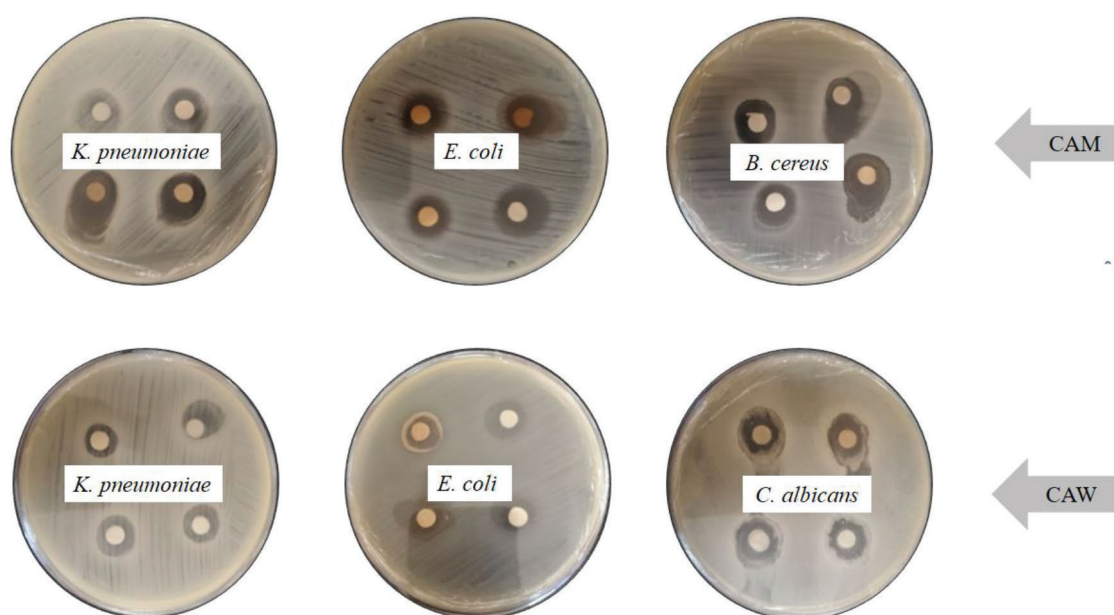


Fig. 10 – Antibacterial activities of CAW and CAM extracts against different bacterial strains

(*Escherichia coli*, *Klebsiella pneumoniae*, *Bacillus cereus*, *Pseudomonas aeruginosa*) and one yeast (*Candida albicans*). For *E. coli*, the aqueous extract produced inhibition zones ranging from 20.66 mm to 11.00 mm, while the methanol extract showed zones from 20.75 mm to 13.50 mm. For *K. pneumoniae*, the aqueous extract ranged from 18.50 mm to 11.25 mm, and the methanol extract ranged from 20.00 mm to 12.00 mm. Regarding *B. cereus*, the aqueous extract produced zones from 16.75 mm to 13.25 mm, whereas the methanol extract varied from 22.75 mm to 12.00 mm. The inhibitory zones for *P. aeruginosa* were 19.75 mm to 11.25 mm for the aqueous extract and 24.00 mm to 12.75 mm for the methanol extract. Lastly, zones measuring between 20.75 mm and 10.50 mm were formed by the aqueous extract for *Candida albicans*, whereas zones measuring between 21.33 mm and 13.25 mm were produced by the methanol extract. Notably, at higher concentrations, the methanol extract demonstrated superior effectiveness compared to the aqueous extract, emphasizing that methanol is a more efficient solvent for isolating the active antimicrobial components from *Carpobrotus acinaciformis* L. However, the results obtained for the aqueous extract are significantly better than those reported in studies by Springfield *et al.*,⁴⁰ who tested against *P. aeruginosa* and *C. albicans* strains, and by Van der Watt *et al.*,¹⁹ who tested against *E. coli*, *K. pneumoniae*, and *P. aeruginosa*. These findings demonstrate strong antimicrobial and antifungal activity for both extracts, with particularly notable efficacy against *P. aeruginosa* and *E. coli*. The relatively low standard deviation in the measurements further reinforces the reliability of these results, confirming the potential of *Carpobrotus acinaciformis* L. as a promising source of natural antimicrobial agents.

Conclusion

This study investigated the antibacterial and anticorrosion properties of *Carpobrotus acinaciformis* leaf extracts, using C1020 carbon steel in a 1 M HCl acid medium. Two extraction methods were employed: methanol extraction (CAM) and water extraction (CAW) at 65 °C. The results demonstrate that both CAW and CAM exhibited significant antibacterial activity and served as effective corrosion inhibitors for C1020 carbon steel in 1 M HCl, with corrosion inhibition efficiencies of 96.01 % for CAM at 350 ppm, and 94.05 % for CAW at 450 ppm, as confirmed by impedance curve analysis. Polarization measurements further indicate that both inhibitors acted as mixed-type inhibitors, with a slight anodic effect. Adsorption of the inhibitors followed the Langmuir adsorption isotherm, and the ΔG_{ads} values revealed that both CAM and CAW ad-

sorbed onto the metal surface through both physical and chemical interactions. Scanning electron microscopy (SEM) analysis of the corrosion products on the C1020 surface exposed to HCl revealed substantial corrosion in the absence of inhibitors, while the presence of CAM and CAW significantly enhanced surface smoothness and reduced corrosion product formation. These findings confirm that both CAM and CAW inhibitors effectively mitigate corrosion of C1020 steel in HCl solutions. Moreover, the study highlights that both CAW and CAM extracts exhibit potent antibacterial activity against *Candida albicans* and four bacterial strains (*Escherichia coli*, *Klebsiella pneumoniae*, *Bacillus cereus* and *Pseudomonas aeruginosa*).

ACKNOWLEDGEMENTS

This research was supported by the Algerian Ministry of Higher Education and Scientific Research (MESRS) under the PRFU project (code: A16N01UN210120230003). The authors would like to express their gratitude to Djareddir Tahar for his invaluable assistance. They also extend their appreciation to the LGCES laboratory team, particularly Professor Mounira Rouania and Sana Ladacyia, for their support.

References

1. Alamri, A. H., Obot, I. B., Highly efficient corrosion inhibitor for C1020 carbon steel during acid cleaning in multi-stage flash (MSF) desalination plant, *Desalination* **470** (2019) 114100. doi: <https://doi.org/10.1016/j.desal.2019.114100>.
2. Ferkous, H., Dilemi, A., Abdennouri, A., Malha, S. I. R., Study of the electrochemical behavior of Al-Zn-In based sacrificial anodes in sea water, *Rev. Sci. Technol.* **29** (2023) 36.
3. Zhang, W., Li, H. J., Liu, Y., Wang, D., Chen, L., Xie, L., Li, L., Zhang, W., Wu, Y. C., Stevioside-Zn²⁺ system as an eco-friendly corrosion inhibitor for C1020 carbon steel in hydrochloric acid solution, *Colloids Surf. A: Physicochem. Eng. Asp.* **612** (2021) 126010. doi: <https://doi.org/10.1016/j.colsurfa.2020.126010>
4. Saremi, M., Dehghanian, C., Sabet, M. M., The effect of molybdate concentration and hydrodynamic effect on mild steel corrosion inhibition in simulated cooling water, *Corros. Sci.* **48** (2006) 1404. doi: <https://doi.org/10.1016/j.corsci.2005.06.009>
5. Alvarez, P. E., Fiori-Bimbi, M. V., Neske, A., Brandán, S. A., Gervasi, C. A., *Rollinia occidentalis* extract as green corrosion inhibitor for carbon steel in HCl solution, *J. Ind. Eng. Chem.* **58** (2018) 92. doi: <https://doi.org/10.1016/j.jiec.2017.09.012>
6. Santos, A. M., Aquino, I. P., Cotting, F., Aoki, I. V., de Melo, H. G., Capelossi, V. R., Evaluation of palm kernel cake powder (*Elaeis Guineensis* Jacq) as corrosion inhibitor for carbon steel in acidic media, *Met. Mater. Int.* **27** (2021) 1519. doi: <https://doi.org/10.1007/s12540-019-00559-x>

7. Gobara, M., Saleh, A., Naeem, I., Synthesis, characterization and application of acrylate-based poly ionic liquid for corrosion protection of C1020 steel in hydrochloric acid solution, *Mater. Res. Express* **7** (2019) 016517. doi: <https://doi.org/10.1088/2053-1591/ab6000>
8. Rizi, A., Sedik, A., Acidi, A., Rachedi, K. O., Ferkous, H., Berredjem, M., Delimi, A., Abdennouri, A., Alam, M., Ernst, B., Benguerba, Y., Sustainable and green corrosion inhibition of mild steel: Insights from electrochemical and computational approaches, *ACS Omega* **8** (2023) 4722. doi: <https://doi.org/10.1021/acsomega.3c06548>
9. Sahraoui, M., Boulkroune, M., Chibani, A., Larbah, Y., Abdessemed, A., Aqueous extract of *Punica granatum* fruit peel as an eco-friendly corrosion inhibitor for aluminium alloy in acidic medium, *J. Bio. Tribo. Corros.* **8** (2022) 54. doi: <https://doi.org/10.1007/s40735-022-00658-0>
10. Bouzana, A., Zohra, C., Bechecker, I., Sakhraoui, N., Bouzenad, N., Chawki, B., Phytochemical analysis by LC MS/MS and in vitro antioxidant activity of the Algerian endemic plant *Dianthus sylvestris* Subsp. *aristidis* (Batt.) Greuter & Burdet, *Glob. Nest. J.* **25** (2023) 113. doi: <https://doi.org/10.30955/gnj.005047>
11. Barreto, L. S., Tokumoto, M. S., Guedes, I. C., Melo, H. G. D., Amado, F. D. R., Capelossi, V. R., Evaluation of the anticorrosion performance of peel garlic extract as corrosion inhibitor for ASTM 1020 carbon steel in acidic solution, *Matéria (Rio J.)* **22** (2017) 3. doi: <https://doi.org/10.1590/S1517-707620170003.0186>
12. Khadom, A. A., Kadhim, M. M., Anaee, R. A., Mahood, H. B., Mahdi, M. S., Salman, A. W., Theoretical evaluation of *Citrus aurantium* leaf extract as green inhibitor for chemical and biological corrosion of mild steel in acidic solution: Statistical, molecular dynamics, docking, and quantum mechanics study, *J. Mol. Liq.* **343** (2021) 116978. doi: <https://doi.org/10.1016/j.molliq.2021.116978>
13. Bouzenad, N., Ammouchi, N., Chaib, N., Belhocine, Y., Belhaoues, A., Hamrouche, N., Boudagha, S. E. L., Abdennouri, A., Zahnit, W., Development of bioplastic films from *Sargassum muticum* alginate: Properties and applications in food packaging, *Iran. J. Chem. Chem. Eng.* **43** (2024) 3794. doi: <https://doi.org/10.30492/ijcce.2024.2023449.6460>
14. Nascimento, G. G. F., Locatelli, J., Freitas, P. C., Silva, G. L., Antibacterial activity of plant extracts and phytochemicals on antibiotic-resistant bacteria, *Braz. J. Microbiol.* **31** (2000) 247. doi: <https://doi.org/10.1590/S1517-8382200000400003>
15. Grigore, M. N., Ivanescu, L., Toma, C., *Halophytes: An Integrative Anatomical Study*, Springer, 2014.
16. Dikilitaş, S. K., Dikilitaş, M., Tıpırdamaz, R., Biochemical and molecular tolerance of *Carpobrotus acinaciformis* L. halophyte plants exposed to high level of NaCl stress, *Harran Tarım ve Gıda Bilimleri Dergisi* **23** (2019) 99. doi: <https://doi.org/10.29050/harranziraat.464133>
17. Traveset, A., Brundu, G., Carta, L., Mprezetou, I., Lambdon, P., Manca, M., Médail, F., Moragues, E., Rodríguez-Pérez, J., Siamantziouras, A. S. D., Suehs, C. M., Troumbis, A. Y., Vilà, M., Hulme, P. E., Consistent performance of invasive plant species within and among Islands of the Mediterranean basin, *Biol. Invasions* **10** (2008) 847. doi: <https://doi.org/10.1007/s10530-008-9245-y>
18. Rostami-Vartooni, A., Nasrollahzadeh, M., Salavati-Niasari, M., Atarod, M., Photocatalytic degradation of azo dyes by titanium dioxide supported silver nanoparticles prepared by a green method using *Carpobrotus acinaciformis* extract, *J. Alloys Compd.* **689** (2016) 15. doi: <https://doi.org/10.1016/j.jallcom.2016.07.253>
19. van der Watt, E., Pretorius, J. C., Purification and identification of active antibacterial components in *Carpobrotus edulis* L., *J. Ethnopharmacol.* **76** (2001) 87. doi: [https://doi.org/10.1016/S0378-8741\(01\)00197-0](https://doi.org/10.1016/S0378-8741(01)00197-0)
20. Kherraf, S., Zouaoui, E., Medjram, M. S., Corrosion inhibition of Monel 400 in hydrochloric solution by some green leaves, *Anti-Corros. Methods Mater.* **64** (2017) 347. doi: <https://doi.org/10.1108/ACMM-05-2016-1673>
21. Kherraf, S., Khelifaoui, M., Boughaita, I., Marsa, Z., Medjram, M. S., Lavandula stoechas as a green corrosion inhibitor for monel 400 in sulfuric acid: Electrochemical, gravimetric, and AFM investigations, *Iran. J. Chem. Chem. Eng.* **42** (2023) 2538. doi: <https://doi.org/10.30492/ijcce.2023.563710.5656>
22. Mechbal, N., Bouhrim, M., Bnouham, M., Hammouti, B., Karzazi, Y., Kaya, S., Serdaroğlu, G., Anticorrosive and antioxidant effect of the aqueous extract of the leaves, flowers, and stems of *Cistus monspeliensis* L.: Experimental and computational study, *J. Mol. Liq.* **331** (2021) 115771. doi: <https://doi.org/10.1016/j.molliq.2021.115771>
23. Rahayu, P. P., Sundari, C. D. D., Farida, I., Corrosion inhibition using lignin of sugarcane bagasse, *IOP Conf. Ser.: Mater. Sci. Eng.* **434** (2018) 012087. doi: <https://doi.org/10.1088/1757-899X/434/1/012087>
24. Muthukumarasamy, K., Pitchai, S., Devarayan, K., Nallathambi, L., Adsorption and corrosion inhibition performance of *Tunbergia fragrans* extract on mild steel in acid medium, *Mater. Today Proc.* **33** (2020) 4054. doi: <https://doi.org/10.1016/j.matpr.2020.06.533>
25. Bouzenad, N., Ammouchi, N., Chaib, N., Messaoudi, M., Bousabaa, W., Bensouici, C., Sawicka, B., Atanassova, M., Ahmad, S. F., Zahnit, W., Exploring bioactive components and assessing antioxidant and antibacterial activities in five seaweed extracts from the Northeastern coast of Algeria, *Mar. Drugs* **22** (2024) 273. doi: <https://doi.org/10.3390/md22060273>
26. de Souza, F. S., Spinelli, A., Caffeic acid as a green corrosion inhibitor for mild steel, *Corros. Sci.* **51** (2009) 642. doi: <https://doi.org/10.1016/j.corsci.2008.12.013>
27. Kahlouche, A., Ferkous, H., Delimi, A., Djellali, S., Yadav, K. K., Fallatah, A. M., Jeon, B. H., Ferial, K., Boulechfar, C., Ben Amor, Y., Benguerba, Y., Molecular insights through the experimental and theoretical study of the anticorrosion power of a new eco-friendly *Cytisus multiflorus* flowers extract in a 1 M sulfuric acid, *J. Mol. Liq.* **347** (2022) 118397. doi: <https://doi.org/10.1016/j.molliq.2021.118397>
28. Zouied, D., Zouaoui, E., Ammouchi, N., Dob, K., Ayadi, M. T., The synergistic effect of acetanilide and para hydroxy acetanilide for corrosion protection of carbon steel in a NaCl medium, *Anal. Bioanal. Electrochem.* **11** (2019) 1329.
29. Fadhil, A. A., Khadom, A. A., Ahmed, S. K., Liu, H., Fu, C., Mahood, H. B., *Portulaca grandiflora* as new green corrosion inhibitor for mild steel protection in hydrochloric acid: Quantitative, electrochemical, surface and spectroscopic investigations, *J. Surf. Interfac.* **20** (2020) 100595. doi: <https://doi.org/10.1016/j.surfin.2020.100595>
30. Şafak, S., Duran, B., Yurt, A., Türkoğlu, G., Schiff bases as corrosion inhibitor for aluminium in HCl solution, *Corros. Sci.* **54** (2012) 251. doi: <https://doi.org/10.1016/j.corsci.2011.09.026>
31. Ammouchi, N., Allal, H., Zouaoui, E., Dob, K., Zouied, D., Bououdina, M., Extracts of *Ruta chalepensis* as green corrosion inhibitor for copper CDA 110 in 3 % NaCl medium: Experimental and theoretical studies, *Anal. Bioanal. Electrochem.* **11** (2019) 830.

32. *Mehdipour, M., Ramezanzadeh, B., Arman, S. Y.*, Electrochemical noise investigation of Aloe plant extract as green inhibitor on the corrosion of stainless steel in 1 M H₂SO₄, *J. Ind. Eng. Chem.* **21** (2015) 318.
doi: <https://doi.org/10.1016/j.jiec.2014.02.041>
33. *Hamed, E., Abd El-REhim, S. S., El-Shahat, M. F., Shaltot, A. M.*, Corrosion inhibition of nickel in H₂SO₄ solution by alanine, *Mater. Sci. Eng. B* **177** (2012) 441.
doi: <https://doi.org/10.1016/j.mseb.2012.01.016>
34. *Dob, K., Zouaoui, E., Zouied, D.*, Corrosion inhibition of curcuma and saffron on A106 Gr B carbon steel in 3 % NaCl medium, *Anti-Corros. Methods Mater.* **65** (2018) 225.
doi: <https://doi.org/10.1108/ACMM-06-2017-1805>
35. *Esmaili, A., Saremnia, B., Kalantari, M.*, Removal of mercury (II) from aqueous solutions by biosorption on the biomass of *Sargassum glaucescens* and *Gracilaria corticata*, *Arab. J. Chem.* **8** (2015) 506.
doi: <https://doi.org/10.1016/j.arabjc.2012.01.008>
36. *Kuznetsov, Yu. I.*, Corrosion inhibitors in conversion coatings. III, *Prot. Met.* **37** (2001) 101.
doi: <https://doi.org/10.1023/A:1010309718379>
37. *Ye, Y., Zou, Y., Jiang, Z., Yang, Q., Chen, L., Guo, S., Chen, H.*, An effective corrosion inhibitor of N doped carbon dots for Q235 steel in 1 M HCl solution, *J. Alloys Compd.* **815** (2020) 152338.
doi: <https://doi.org/10.1016/j.jallcom.2019.152338>
38. *Benabbouha, T., Siniti, M., Byadi, S., Chefira, K., El Attari, H., Barhoumi, A., Chafi, M., Chibi, F., Rchid, H., Rachid, N.*, Insight into corrosion inhibition mechanism of carbon steel by an algal extract as an eco-friendly corrosion inhibitor in 0.5 M H₂SO₄: Experimental and molecular dynamics study, *Mater. Corros.* **74** (2023) 1535.
doi: <https://doi.org/10.1002/maco.202313907>
39. *Alsabagh, A. M., Migahed, M. A., Awad, H. S.*, Reactivity of polyester aliphatic amine surfactants as corrosion inhibitors for carbon steel in formation water (deep well water), *Corros. Sci.* **48** (2006) 813.
doi: <https://doi.org/10.1016/j.corsci.2005.04.009>
40. *Springfield, E. P., Amabeoku, G., Weitz, F., Mabusela, W., Johnson, Q.*, An assessment of two *Carpobrotus* species extracts as potential antimicrobial agents, *Phytomedicine* **10** (2003) 434.
doi: <https://doi.org/10.1078/0944-7113-00263>